Description of Model and Codes

Impaired Myocardial Energetics Causes Mechanical Dysfunction in Decompensated Failing Hearts

Rachel Lopez[1]; Bahador Marzban[1]; Xin Gao[1]; Ellen Lauinger[1]; Françoise Van den Bergh[1]; Steven E. Whitesall[2]; Kimber Converso-Baran[2]; Charles F. Burant[1,3]; Daniel E. Michele[1,2]; Daniel A. Beard[1]

[1]Department of Molecular and Integrative Physiology, University of Michigan, Ann Arbor, MI

[2]Frankel Cardiovascular Center Physiology and Phenotyping Core, University of Michigan, Ann Arbor, MI

[3]Department of Internal Medicine, University of Michigan, Ann Arbor, MI

1. Model of Cardiac Energy Metabolism

Model Variables:

The cellular energy metabolism model is based on the mitochondrial oxidative phosphorylation model of Bazil et al. [1]. The model is governed by 29 ordinary differential equations governing mitochondrial membrane potential, metabolite species concentrations, and cation (H^+, K^+, and Mg^{2+}) concentrations in the mitochondrial matrix, inter-membrane space, and cytosol. Table S1.1 lists the state variables of the model, with a brief description, units used in the model, and the variable name used in the model codes. The original formulation of the model accounted for reactive oxygen species $O_2^{\cdot-}$ and H_2O_2, which are ignored here, and thus the model is modified accordingly from [1].

Table S1.1. Energetics Model State Variables

State Variable	Definition	Units used in code	Variable name in code
$\Delta\Psi$	Mitochondrial membrane potential	mV	DPsi_im_to_matrix
Mitochondrial Matrix State Variables			
$[ATP]_x$	Total matrix ATP concentration	M	ATP_matrix
$[ADP]_x$	Total matrix ADP concentration	M	ADP_matrix
$[Pi]_x$	Total matrix Pi concentration	M	Pi_matrix
$[NADH]_x$	Total matrix NADH concentration	M	NADH_matrix
$[NAD]_x$	Total matrix NAD concentration	M	NAD_matrix
$[UQH_2]_x$	Total matrix ubiquinol concentration	M	coQH2_matrix
$[UQ]_x$	Total matrix ubiquinone concentration	M	coQ_matrix
$[H^+]_x$	Matrix free proton concentration	M	h_matrix
$[K^+]_x$	Matrix free potassium concentration	M	k_matrix
$[Mg^{2+}]_x$	Matrix free magnesium concentration	M	m_matrix
Intermembrane Space (IMS) State Variables			

$[c^{2+}]_i$	Total IMS cytochrome c^{2+} (reduced) concentration	M	cytocred_im
$[c^{3+}]_i$	Total IMS cytochrome c^{3+} (oxidized) concentration	M	cytocox_im
$[ATP]_i$	Total IMS ATP concentration	M	ATP_ im
$[ADP]_i$	Total IMS ADP concentration	M	ADP_ im
$[AMP]_i$	Total IMS AMP concentration	M	AMP_im
$[Pi]_i$	Total IMS Pi concentration	M	Pi_ im
$[H^+]_i$	IMS free proton concentration	M	h_im
$[K^+]_i$	IMS free potassium concentration	M	k_im
$[Mg^{2+}]_i$	IMS free magnesium concentration	M	m_im
Cytosolic State Variables			
$[ATP]_c$	Total cytosolic ATP concentration	M	ATP_c
$[ADP]_c$	Total cytosolic ADP concentration	M	ADP_c
$[AMP]_c$	Total cytosolic AMP concentration	M	AMP_c
$[Pi]_c$	Total cytosolic Pi concentration	M	Pi_c
$[CrP]_c$	Total cytosolic creatine phosphate concentration	M	phosphocreatine_c
$[Cr]_c$	Total cytosolic creatine concentration	M	creatine_c
$[H^+]_c$	Cytosolic free proton concentration	M	h_c
$[K^+]_c$	Cytosolic free potassium concentration	M	k_c
$[Mg^{2+}]_c$	Cytosolic free magnesium concentration	M	m_c

The governing equations for these variables are delineated below.

Mitochondrial Membrane Potential:

The potential difference across the mitochondrial inner membrane is governed by currents across the membrane:

$$\frac{d\Delta\Psi}{dt} = (4J_{C1} + 2J_{C3} + 4J_{C4} - nH_{F1F0}J_{F1F0} - J_{ANT} - J_{Hleak})/C_{mito} \qquad (1.1)$$

where J_{C1}, J_{C3}, and J_{C4}, are the complex I, III, and IV fluxes, which are associated with pumping 4, 2, and 4 positive charges out of the matrix. The F_1F_0 ATPase turnover rate is J_{F1F0} and nH_{F1F0} (= 3/8) is the proton flux stoichiometric number associated with the synthesis of one ATP. The fluxes J_{ANT} and J_{Hleak} are the adenine nucleotide translocator and proton leak fluxes.

Mitochondrial Matrix Metabolite State Variables:

Metabolite *concentrations* in the matrix are governed by:

$$\frac{d[ATP]_x}{dt} = (J_{F1F0} - J_{ANT})/Vol_x$$

$$\frac{d[ADP]_x}{dt} = (J_{ANT} - J_{F1F0})/Vol_x$$

$$\frac{d[Pi]_x}{dt} = (J_{PIC} - J_{F1F0})/Vol_x$$

$$\frac{d[\text{NAD}]_x}{dt} = (J_{C1} - J_{DH})/Vol_x$$

$$\frac{d[\text{NADH}]_x}{dt} = (J_{DH} - J_{C1})/Vol_x$$

$$\frac{d[\text{UQ}]_x}{dt} = (J_{C3} + \alpha_{C2}J_{DH} - J_{C1})/Vol_x$$

$$\frac{d[\text{UQH}_2]_x}{dt} = (-J_{C3} - \alpha_{C2}J_{DH} + J_{C1})/Vol_x \tag{1.2}$$

where Vol_x is the water volume of the mitochondrial matrix in units of volume of matrix water space per unit mitochondrial volume, the fluxes in the right-hand sides of these expressions are in units of moles per unit liter of mitochondrial volume per unit time, and are defined below.

Inter-Membrane Space (IMS) Metabolite State Variables:

Metabolite concentrations in the intermembrane space are governed by:

$$\frac{d[\text{c}^{2+}]_i}{dt} = (-2J_{C4} + 2J_{C3})/Vol_i$$

$$\frac{d[\text{c}^{3+}]_i}{dt} = (2J_{C4} - 2J_{C3})/Vol_i$$

$$\frac{d[\text{ATP}]_i}{dt} = (J_{ANT} + J_{ATPPERM})/Vol_i$$

$$\frac{d[\text{ADP}]_i}{dt} = (-J_{ANT} + J_{ADPPERM})/Vol_i$$

$$\frac{d[\text{AMP}]_i}{dt} = (J_{AMPPERM})/Vol_i$$

$$\frac{d[\text{Pi}]_i}{dt} = (-J_{PIC} + J_{PIPERM})/Vol_i \tag{1.3}$$

where Vol_i is the water volume of the mitochondrial inter-membrane space in units of volume of IMS water space per unit mitochondrial volume, the fluxes in the right-hand sides of these expressions are in units of moles per unit liter of mitochondrial volume per unit time, and are defined below.

Cytosolic Metabolite State Variables:

Metabolite concentrations in the cytosolic space are governed by:

$$\frac{d[\text{ATP}]_c}{dt} = \left(-J_{ATPase} + J_{CK} + J_{AK} - J_{ATPPERM}\frac{V_{Rm}}{V_{Rc}}\right)/Vol_c$$

$$\frac{d[\text{ADP}]_c}{dt} = \left(+J_{ATPase} - J_{CK} - 2J_{AK} - J_{ADPPERM}\frac{V_{Rm}}{V_{Rc}}\right)/Vol_c$$

$$\frac{d[\text{AMP}]_c}{dt} = \left(+J_{AK} - J_{AMPPERM}\frac{V_{Rm}}{V_{Rc}}\right)/Vol_c$$

$$\frac{d[\text{Pi}]_c}{dt} = \left(+J_{ATPase} - J_{PIPERM}\frac{V_{Rm}}{V_{Rc}}\right)/Vol_c$$

$$\frac{d[\text{CrP}]_c}{dt} = (-J_{CK})/Vol_c$$

$$\frac{d[\text{Cr}]_c}{dt} = (+J_{AK})/Vol_c \tag{1.4}$$

where Vol_c is the water volume of the cytosolic space in units of volume of cytosolic water space per unit cell volume. The fluxes in the right-hand sides of these expressions are defined below. The ratio V_{Rm}/V_{Rc} is ratio of regional volume of the IMS to the cytosolic space. Since the $J_{ATPPERM}, J_{ADPPERM},$

$J_{AMPPERM}$, and J_{PIPERM} fluxes are in units of mass per unit time per unit mitochondrial volume, the multiplication by V_{Rm}/V_{Rc} converts the units to mass per unit time per unit cytosolic volume. The units of the other fluxes (cytosolic reaction fluxes) are mass per unit time per unit cytosolic volume.

Cation Concentration State Variables:

The governing equations for the cation (H^+, K^+, and Mg^{2+}) concentrations in the mitochondrial and extra-mitochondrial compartments are derived using the method outlined in Vinnakota et al. [2]. In brief, the equations account for rapid equilibria between conjugate bases of biochemical weak acid species (e.g., ATP^{4-}) and cation bound species (e.g., $HATP^{3-}$, $KATP^{3-}$, and $MgATP^{2-}$). The full set of equations is detailed in the supplementary material published with Bazil et al. [1].

Energetic Model Fluxes:

The fluxes on the right-hand sides of Equations (1.1)-(1.4) are defined in Table S1.2.

Table S1.2. Energetics Model Reaction and Transport Fluxes

Flux	Definition	Units used in code	Variable name in code
J_{C1}	Electron transport chain Complex I flux	mole·sec^{-1}·(l mito)$^{-1}$	J_ETC1_im_to_matrix
J_{C3}	Electron transport chain Complex III flux	mole·sec^{-1}·(l mito)$^{-1}$	J_ETC3_im_to_matrix
J_{C4}	Electron transport chain Complex IV flux	mole·sec^{-1}·(l mito)$^{-1}$	J_ETC4_im_to_matrix
J_{F1F0}	Mitochondrial F_1F_0 ATPase flux	mole·sec^{-1}·(l mito)$^{-1}$	J_F1F0ATPASE_im_to_matrix
J_{ANT}	Adenine nucleotide translocase flux	mole·sec^{-1}·(l mito)$^{-1}$	J_ANT_im_to_matrix
J_{Hleak}	Proton leak flux	mole·sec^{-1}·(l mito)$^{-1}$	J_HLEAK_im_to_matrix
J_{DH}	Rate of NADH production	mole·sec^{-1}·(l mito)$^{-1}$	J_DH_matrix
J_{PIC}	Mitochondrial phosphate carrier flux	mole·sec^{-1}·(l mito)$^{-1}$	J_PIH_im_to_matrix
$J_{ATPPERM}$	Mitochondrial outer membrane ATP permeability	mole·sec^{-1}·(l mito)$^{-1}$	J_ATPPERM_cytoplasm_to_im
$J_{ADPPERM}$	Mitochondrial outer membrane ADP permeability	mole·sec^{-1}·(l mito)$^{-1}$	J_ADPPERM_cytoplasm_to_im
$J_{AMPPERM}$	Mitochondrial outer membrane AMP permeability	mole·sec^{-1}·(l mito)$^{-1}$	J_AMPPERM_cytoplasm_to_im
J_{PIPERM}	Mitochondrial outer membrane Pi permeability	mole·sec^{-1}·(l mito)$^{-1}$	J_PIPERM_cytoplasm_to_im
J_{CK}	Cytosolic creatine kinase flux	mole·sec^{-1}·(l cytosol)$^{-1}$	J_AK_cytoplasm
J_{AK}	Cytosolic adenylate kinase flux	mole·sec^{-1}·(l cytosol)$^{-1}$	J_CK_cytoplasm
J_{ATPase}	Cytosolic ATP hydrolysis flux	mole·sec^{-1}·(l cytosol)$^{-1}$	J_ATPASE_cytoplasm

The mathematical expressions for these fluxes are detailed in Bazil et al. [1].

Implementation in Multiscale Model:

The cellular energetics model is implemented in a MATLAB script called EnergeticsModelScript.m. This script is used to predict cytosolic [ATP], [ADP], [AMP], [Pi], [Cr], and [CrP] at a specified input rate of cytosolic ATP hydrolysis. Input and output arguments for the script are listed below in Tables S1.3 and S1.4.

Table S1.3. Input arguments for cellular energetics model

Input variable	Definition	Units used in code	Values
TAN	total adenine nucleotide pool	$mole \cdot (l\ cell)^{-1}$	0.0071-0.0086 for sham 0.0052-0.0085 for TAC
CRtot	total creatine pool	$mole \cdot (l\ cell)^{-1}$	0.0267-0.0330 for sham 0.0146-0.0278 for TAC
TEP	total exchangeable phosphate pool	$mole \cdot (l\ cell)^{-1}$	0.0247-0.0298 for sham 0.0181-0.0293 for TAC
Ox_capacity	oxidative capacity (relative to control)	unitless	0.834-1.1526 for sham 0.5287-0.9755 for TAC
x_ATPase	ATP hydrolysis rate	$mmole \cdot sec^{-1} \cdot (l\ cytosol)^{-1}$	1.5202-2.2257 for sham 1.1009-2.2504 for TAC

Table S1.4. Output arguments for cellular energetics model

Output variable	Definition	Units used in code	Values
MgATP_cytoplasm	cytosolic [MgATP]	$mmole \cdot (l\ cytosol\ water)^{-1}$	7.2308-9.4533 for sham 4.9443-9.0718 for TAC
MgADP_cytoplasm	cytosolic [MgADP]	$mmole \cdot (l\ cytosol\ water)^{-1}$	0.0408-0.0525 for sham 0.0235-0.0485 for TAC
fPi_cytoplasm	cytosolic unchelated [Pi]	$mmole \cdot (l\ cytosol\ water)^{-1}$	0.3657-1.1464 for sham 1.0785-1.5613 for TAC
MVO2_tissue	oxygen consumption rate	$\mu mol \cdot min^{-1} \cdot (g\ tissue)^{-1}$	8.5402-13.2541 for sham 7.6718-14.0538 for TAC
dGrATPase	ATP hydrolysis rate	$kJ \cdot mole^{-1}$	-(66.767-63.418) for sham -(64.042-62.345) for TAC
PCrATP	CrP/ATP ratio	unitless	2.073-2.613 for sham 1.687-2.169 for TAC
ATP_cyto	cytosolic total [ATP]	$mmole \cdot (l\ cytosol\ water)^{-1}$	8.750-11.453 for sham 5.992-10.978 for TAC
ADP_cyto	cytosolic total [ADP]	$mmole \cdot (l\ cytosol\ water)^{-1}$	0.1015-0.1307 for sham 0.0588-0.1205 for TAC
Pi_cyto	cytosolic total [Pi]	$mmole \cdot (l\ cytosol\ water)^{-1}$	0.6132-1.92 for sham 1.808-2.621 for TAC

2. Cardiomyocyte Mechanics Model

Model Variables and Equations:

A cardiomyocyte mechanics model based on the models of Tewari et al. [3, 4] and Campbell et al. [5] is used to simulate the active and passive components of myocardial wall tension used in the heart model (§3, below) and to determine the ATP hydrolysis rate used in the energy metabolism model (§1, above). The components of the model are illustrated in Fig. S1.
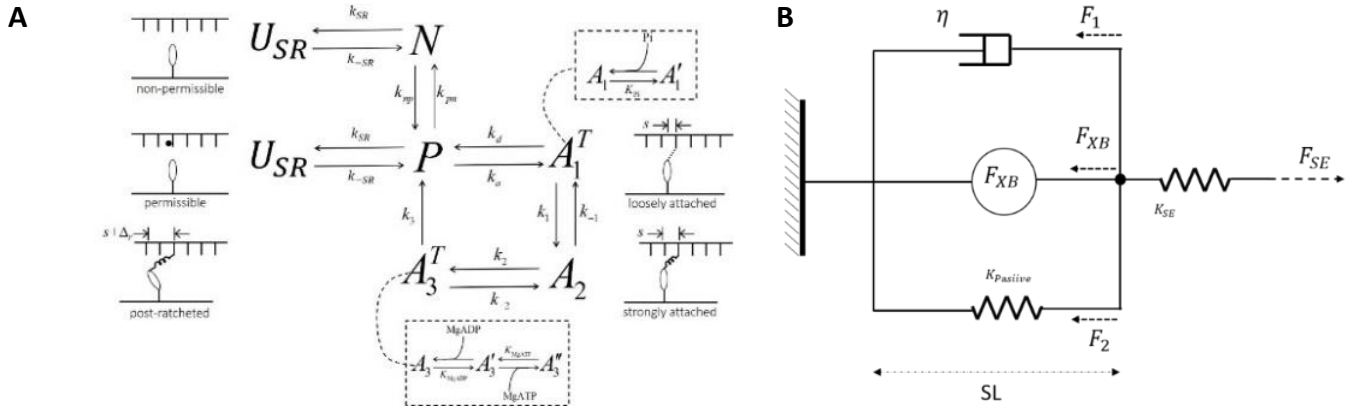
Fig. S1. Cardiomyocyte mechanics model. The multi-scale strain-dependent model for the cross-bridge cycle is illustrated in panel A. The integration of the cross-bridge for (F_{XB}) into a model of muscle mechanics is illustrated in panel B.

The five states in the cross-bridge model correspond to: the non-permissible (no calcium bound) state N, the permissible (calcium-bound) state P, loosely attached state A_1, strongly attached state A_2, and post-ratcheted state A_3. The attached states are distributed over a continuum of cross-bridge strain. To numerically simulate the model a moment-expansion approach is used where ordinary differential equations for the first three moments of the probability distributions of strain of each of the attached states are simulated.

The state variables for the cross-bridge model are tabulated below.

Table S2.1. State variables in cross-bridge model

State Variable	Definition	Units used in code	Variable name in code
p_1^0	The 0th moment of state A_1 strain probability distribution. Equal to the proportion of cross-bridges in state A_1.	unitless	P1_0
p_1^1	The 1st moment of state A_1 strain probability distribution.	μm	P1_1
p_1^2	The 2nd moment of state A_1 strain probability distribution.	μm^2	P1_2
p_2^0	The 0th moment of state A_2 strain probability distribution. Equal to the proportion of cross-bridges in state A_2.	unitless	P2_0
p_2^1	The 1st moment of state A_2 strain probability distribution.	μm	P2_1
p_2^2	The 2nd moment of state A_2 strain probability distribution.	μm^2	P2_2
p_3^0	The 0th moment of state A_3 strain probability distribution. Equal to the proportion of cross-bridges in state A_3.	unitless	P3_0
p_3^1	The 1st moment of state A_3 strain probability distribution.	m	P3_1
p_3^2	The 2nd moment of state A_3 strain probability distribution.	μm^2	P3_2

N	Non-permissible XB state	unitless	N
U_{NR}	Non relaxed state	unitless	U_NR

The equations used to simulate the cross-bridge model are

$$\frac{dp_1^0}{dt} = k_a P(t) U_{NR} OV_{thick} - \widetilde{k_d}p_1^0 - \widetilde{k_1}\left(p_1^0 - \alpha_1 p_1^1 + \frac{1}{2}\alpha_1^2 p_1^2\right) + k_{-1}(p_2^0 + \alpha_1 p_2^1 + \frac{1}{2}\alpha_1^2 p_2^2)$$

$$\frac{dp_1^1}{dt} = v\,p_1^0 - \widetilde{k_d}p_1^1 - \widetilde{k_1}(p_1^1 - \alpha_1 p_1^2) + k_{-1}(p_2^1 + \alpha_1 p_2^2)$$

$$\frac{dp_1^2}{dt} = 2vp_1^1 - \widetilde{k_d}p_1^2 - \widetilde{k_1}p_1^2 + k_{-1}p_2^2$$

$$\frac{dp_2^0}{dt} = \widetilde{k_1}\left(p_1^0 - \alpha_1 p_1^1 + \frac{1}{2}\alpha_1^2 p_1^2\right) - k_{-1}(p_2^0 + \alpha_1 p_2^1 + \frac{1}{2}\alpha_1^2 p_2^2) - k_2\left(p_2^0 - \alpha_2 p_2^1 + \frac{1}{2}\alpha_2^2 p_2^2\right) + \widetilde{k_{-2}}p_3^0$$

$$\frac{dp_2^1}{dt} = v\,p_2^0 + \widetilde{k_1}(p_1^1 - \alpha_1 p_1^2) - k_{-1}(p_2^1 + \alpha_1 p_2^2) - k_2(p_2^1 - \alpha_2 p_2^2) + \widetilde{k_{-2}}p_3^1$$

$$\frac{dp_2^2}{dt} = 2v\,p_2^1 + \widetilde{k_1}p_1^2 - k_{-1}p_2^2 - k_2 p_2^2 + \widetilde{k_{-2}}p_3^2$$

$$\frac{dp_3^0}{dt} = k_2\left(p_2^0 - \alpha_2 p_2^1 + \frac{1}{2}\alpha_2^2 p_2^2\right) - \widetilde{k_{-2}}p_3^0 - \widetilde{k_3}(p_3^0 - \alpha_3 s_3^2 p_3^0 + 2\alpha_3 s_3 p_3^1 + p_3^2)$$

$$\frac{dp_3^1}{dt} = v\,p_3^0 + k_2(p_2^1 - \alpha_2 p_2^2) - \widetilde{k_{-2}}p_3^1 - \widetilde{k_3}(p_3^1 - \alpha_3 s_3^2 p_3^1 + 2\alpha_3 s_3 p_3^2)$$

$$\frac{dp_3^2}{dt} = 2v\,p_3^1 + k_2 p_2^2 - \widetilde{k_{-2}}p_3^2 - \widetilde{k_3}(p_3^2 + \alpha_3 s_3^2 p_3^2) \tag{2.1}$$

where v is the velocity of sliding ($v = dSL/dt$ where SL is the sarcomere length, used below in the heart model of §3).

Metabolite concentrations affect the apparent rate constants in the model via the following relations:

$$\widetilde{k_d} = k_d \frac{\frac{[Pi]}{K_{Pi}}}{1 + \frac{[Pi]}{K_{Pi}}}$$

$$\widetilde{k_1} = k_1 \frac{1}{1 + \frac{[Pi]}{K_{Pi}}}$$

$$\widetilde{k_{-2}} = k_{-2} \frac{\frac{[MgADP]}{K_{MgADP}}}{1 + \frac{[MgADP]}{K_{MgADP}} + \frac{[MgATP]}{K_{MgATP}}}$$

$$\widetilde{k_3} = k_3 \frac{\frac{[MgATP]}{K_{MgATP}}}{1 + \frac{[MgADP]}{K_{MgADP}} + \frac{[MgATP]}{K_{MgATP}}} \tag{2.2}$$

A detailed description of the moment expansion and associated equations is given in Tewari et al. [4].

Calcium activation:

The calcium activation model is adopted from Campbell et al. [6] model with minor modifications. The equations for calcium-mediated transition from the N to the P state are:

$$J_{on} = k_{on} [Ca^{2+}] N \left(1 + k_{coop}(1 - N)\right) \tag{2.3}$$

$$J_{off} = k_{off} P \left(1 + k_{coop} N\right) \tag{2.4}$$

The $k_{coop}(1 - N)$ is representative of cooperative activation.

The variable N represents the non-permissible state:

7

$$P = 1 - N - p_1^0 - p_2^0 - p_3^0 \tag{2.5}$$

$$\frac{dN}{dt} = -J_{on} + J_{off} \tag{2.6}$$

where P is the permissible (calcium-bound).

Super-relaxed state:

The Campbell et al. model for calcium activation includes a transition between a super-relaxed and not relaxed state.

$$U_{SR} \leftrightarrow U_{NR}$$

$$U_{SR} + U_{NR} = 1 \tag{2.6}$$

where the transition from super-relaxed (U_{SR}) to non-relaxed (U_{NR}) state is force-dependent:

$$\frac{dU_{NR}}{dt} = k_{SR}\left(1 + k_{force}\ OV_{thick}\ F_{XB}\right)U_{SR} - k_{-SR}\ U_{NR}\ . \tag{2.7}$$

Overlap function:

Following Rice et al. [7] fractional overlap between thin and thick filament is represented as follows:

$$OV_{Z-axis} = \min\left(\frac{L_{thick}}{2}, \frac{SL}{2}\right)$$

where OV_{Z-axis} is the overlap region closest to the Z-axis.

$$OV_{M-line} = \max\left(\frac{SL}{2} - (SL - L_{thin}), \frac{L_{bare}}{2}\right)$$

where OV_{M-line} is the overlap region closest to the M-line. The length of overlap LOV can be computed as following:

$$LOV = OV_{Z-axis} - OV_{M-line}$$

Using length of overlap LOV, fraction of thick filament overlap is computed as following:

$$OV_{thick} = \frac{2LOV}{L_{thick} - L_{bare}} \tag{2.8}$$

Here SL is the length of sarcomere. L_{thick}, L_{thin}, L_{bare} are the length of thick filament, bare region of the thick filament and, the length of the thin filament, respectively.

Table S2.2. Sarcomere overlap function parameters

Parameter	Definition	Value and units	Parameter name in code
L_{thin}	Thin filament length	1200 nm	L_thin
L_{thick}	Thick filament length	1670 nm	L_thick
L_{bare}	Bare length of the thick filament	100 nm	L_hbare
OV_{Z-axis}	overlap region closest to the Z-axis	nm	sovr_ze
OV_{M-line}	overlap region closest to the M-line	nm	sovr_cle
LOV	length of overlap LOV	nm	L_sovr
OV_{thick}	fraction of thick filament overlap	unitless	N_overlap

Active and passive force:

The active force generated by cross-bridges is computed from contributions from pre- and post-ratcheted states:

$$\sigma_{XB}(t) = OV_{thick} \, k_{stiff,1} \, (p_2^2 + p_3^2) + k_{stiff,2} \, \Delta r \, p_3^0 \tag{2.9}$$

where $k_{stiff,1}$ and $k_{stiff,2}$ are stiffness constants, Δr is the cross bridge strain associated with ratcheting deformation.

The full muscle model (Fig. 2.1B) includes contributions from the active force generated by the cross-bridge mechanics, the viscous and passive forces associated with the muscle, F_1 and F_2, and a series element force F_{SE}. Overall force balance for the model yields

$$\sigma_{SE}(t) = \sigma_{XB}(t) + \sigma_1(t) + \sigma_2(t). \tag{2.10}$$

The stress contributed from the dashpot (viscous) is determined from the rate of change of sarcomere length

$$\sigma_1 = \eta \frac{dSL}{dt} \tag{2.11}$$

The passive force σ_2 is a function of sarcomere length and is calculated

$$\sigma_2 \, (SL) = K_{Passive} \, (SL - SL_{rest}) + \sigma_{Passive\_collagen} \tag{2.12}$$

where $K_{Passive}$ is the stiffness parameters for the passive force. SL_{rest} is the sarcomere rest length.

$$\sigma_{Passive\_collagen} \, (SL) = \begin{cases} \beta . K_{Passive} \left[e^{\left(PExp_{collagen}(SL - SL_{collagen}) \right)} - 1 \right] \; if \; SL > SL_{collagen} \\ 0 \; if \; SL < SL_{collagen} \end{cases} \tag{2.13}$$

Model Parameters:

Certain parameters from the cross-bridge and calcium-activation models of Tewari et al. [3, 4] and Cambell et al. [6] were re-estimated to match data from [8] on calcium transients and force-generation in isolated rat cardiac trabeculae. In brief, experiments were conducted at 37° C. Calcium transients (Fig. S2A) were measured at different stimulation frequencies at fixed sarcomere length SL = 2.2 μm. Isometric tension time courses were measured at different stimulation frequencies and sarcomere lengths. Fig. S2B shows data on peak developed tension (T_{dev}) as a function of SL at stimulation frequency of 4 Hz; and data on relaxation time from peak to 50% of peak tension (RT50); peak developed tension (T_{dev}) and time to peak tension (TPP) as function of SL.

Model simulations were fit to these data to estimate unknown parameters in the calcium activation and cross-bridge kinetics components of the model. Specifically, parameters adjusted to values different from those in the original publication are indicated below in Table S2.2.
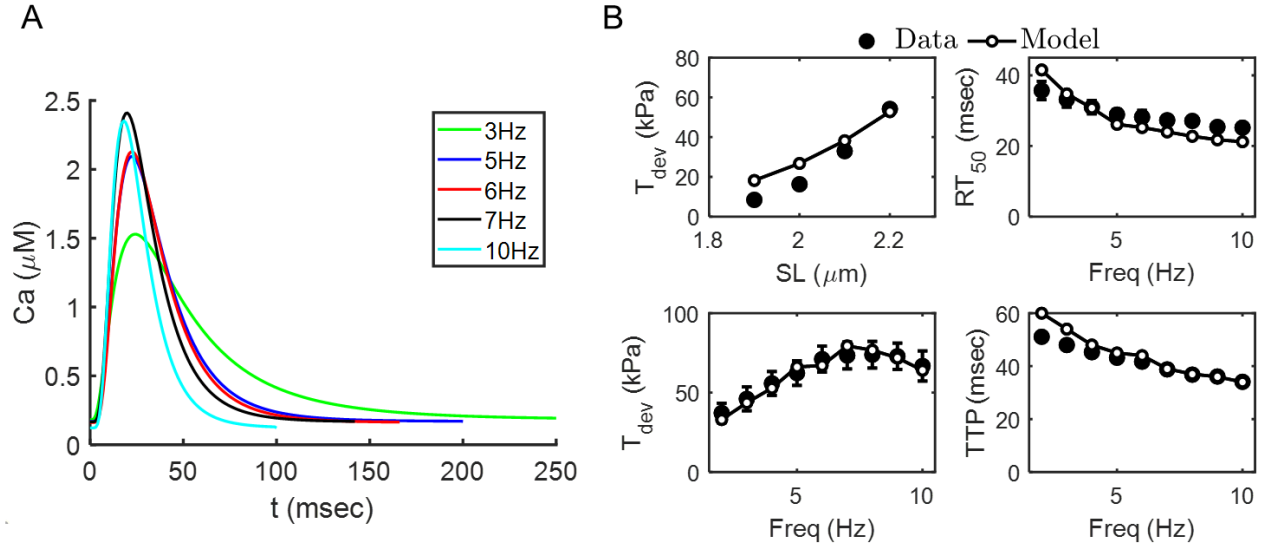
Fig S2. Crossbridge model parameters estimation. For SL =1.9 um the Ca50 = 5.89 and n = 4.63 and for SL = 2.3 um the Ca50 = 6.001 and n = 4.47.

Table S2.2. Model parameters for cross bridge model

Parameters	Definition	Value and units	Parameter name in code	Reference
K_{Stiff1}	Stiffness constant of frictional forces arising due to myosin–actin interaction	13907 mmHg/μm	kstiff2	Fit to data in Fig. S2
K_{Stiff2}	Stiffness constant of forces arising due to working stroke of XBs	341590 mmHg/μm	kstiff1	Fit to data in Fig. S2
$K_{passive}$	Stiffness constant associated with the passive model adopted from Campbell et al.	43 mmHg/μm	k_passive	Fit to data in Fig. S2
$L_{0\_passive}$	Sarcomere length at which passive force is zero	1.8 μm	L_rest_passive	Campbell et al.
α_1	Stretch-sensing parameter for k_1 and k_{-1}	10 μm^{-1}	alpha1	Tewari et al.
α_2	Stretch-sensing parameter for k_2	9 μm^{-1}	alpha2	Tewari et al.
α_3	Stretch-sensing parameter for k_3	5.93 μm^{-1}	alpha3	Fit to data in Fig. S2
s_3	Stretch in state A_3^T at which k_3 is minimum	0.0099 nm	s3	Tewari et al.
k_{coop}	strength of thin filament cooperativity	1.857	K_coop	Fit to data in Fig. S2
k_{on}	Ca on rate - binding to troponin C	101.185 μM^{-1} s^{-1}	k_on	Fit to data in Fig. S2

k_{off}	Ca off rate - binding to troponin C	$723.85\ \text{s}^{-1}$	k_off	Fit to data in Fig. S2
k_{force}	Model parameter for force dependent super relax transition	$1.1688 \times 10^{-3}\ \text{N}^{-1}\text{m}^{-2}$	kforce	Fit to data in Fig. S2
k_{SR}	On rate constant for super relax state	$14.4409\ \text{s}^{-1}$	k1sr	Fit to data in Fig. S2
k_{-SR}	Off rate constant for super relax state	$50.032\ s^{-1}$	K2sr	Fit to data in Fig. S2
k_{MgATP}	[MgATP] dissociation constant	489.7 μM	K_T	Tewari et al.
k_{MgADP}	[MgADP] dissociation constant	0.194 mM	K_D	Tewari et al.
k_{Pi}	[Pi] dissociation constant	4.0 mM	K_Pi	Tewari et al.
k_a	Myosin–actin rate of attachment	$559.5568\ \text{s}^{-1}$	ka	Fit to data in Fig. S2
k_d	Myosin–actin rate of un-attachment	$304.6708\ \text{s}^{-1}$	kd	Fit to data in Fig. S2
k_1	Rate of partially-bound conformation to strongly-bound conformation	$112.3727\ \text{s}^{-1}$	k1	Fit to data in Fig. S2
k_{-1}	Rate of strongly-bound conformation to partially-bound conformation	$21.296\ \text{s}^{-1}$	km1	Tewari et al.
k_2	Rate of ratcheting	$811.72\ \text{s}^{-1}$	k2	Tewari et al.
k_{-2}	Rate of un-ratcheting	$43.25\ \text{s}^{-1}$	km2	Tewari et al.
k_3	Myosin–actin detachment rate	$144.5586\ \text{s}^{-1}$	k3	Fit to data in Fig. S2

3. Heart Model

Model Variables and Equations:

A modified version of the Lumens et al. [9] TriSeg model is used to simulate left- and right-ventricular mechanics, based on the implementation of Tewari et al. [3]. Tension development in each of the left-ventricular free wall, septum, and right-ventricular free wall is simulated using a cell mechanics model to represent each of these segments. From Eqs. (2.9) and (2.13) the rates of change of sarcomere length in these three segments is given by

$$\frac{dSL_{RV}}{dt} = \frac{\sigma_{SE,RV} - \sigma_2(SL_{RV}) - \lambda_{XB}\sigma_{XB,RV}(t)}{\eta}$$

$$\frac{dSL_{LV}}{dt} = \frac{\sigma_{SE,LV} - \sigma_2(SL_{LV}) - \lambda_{XB}\sigma_{XB,LV}(t)}{\eta}$$

$$\frac{dSL_{SEP}}{dt} = \frac{\sigma_{SE,SEP} - \sigma_2(SL_{SEP}) - \lambda_{XB}\sigma_{XB,SEP}(t)}{\eta} \tag{3.1}$$

where the parameter λ_{XB} is a scalar used to account for differences in force generation in vivo versus in vitro. (The value $\lambda_{XB} = 1.31$, determined by Tewari et al. [3] accounts for slightly lower force generation in vitro versus in vivo.) The SL and dSL/dt computed from Eq. (3.1) are used in Eqs. (2.1) which govern cross-bridge dynamics in each segment. The dynamical state of the cross-bridge model in each segment, in turn, appears in Eq. (3.1), which governs $SL(t)$ for each segment.

The series element elastic force for each segment is computed to be proportional to the difference between the sarcomere length and the sarcomere length calculated from natural myofiber strain:

11

$$\sigma_{SE,RV} = K_{SE}(SL_{0,RV} - SL_{RV})$$

$$\sigma_{SE,LV} = K_{SE}(SL_{0,LV} - SL_{LV})$$

$$\sigma_{SE,SEP} = K_{SE}(SL_{0,SEP} - SL_{SEP})$$

where

$$SL_{0,\#} = SL_{ref}\exp(\varepsilon_f)$$

$$\varepsilon_f = \frac{1}{2}\ln\left(\frac{A_{m,\#}}{A_{m,ref,\#}}\right) - \frac{1}{12}z^2 - 0.019z^4; \qquad z_{\#} = \frac{3C_{m,\#}V_{w,\#}}{2A_{m,\#}}$$

$$V_{m,\#} = \frac{\pi}{6}x_{m,\#}(x_{m,\#}^2 + 3y_m^2); \quad A_{m,\#} = \pi(x_{m,\#}^2 + y_m^2); \qquad C_{m,\#} = \frac{2x_{m,\#}}{x_{m,\#}^2 + y_m^2}$$

Here, $A_{m,\#}$ is the midwall surface area of segment #, $A_{m,ref,\#}$ is a reference midwall surface area, $C_{m,\#}$ is the curvature of the midwall surface, $V_{w,\#}$ is the wall volume of wall segment #, $V_{m,\#}$ is the midwall volume, and $x_{m,\#}$ and y_m determine the geometry of the LV and RV cavity (see [9]). The four variables of the TriSeg heart model, $x_{m,RV}$, $x_{m,LV}$, $x_{m,SEP}$, and y_m that determine the geometry of the ventricular cavities, are listed in Table S3.1.

Table S3.1. State variables in TriSeg (Heart) model

State Variable	Definition	Units used in code	Variable name in code
$x_{m,RV}$	Maximal axial distance from RV midwall surface to origin	cm	Xm_RV
$x_{m,LV}$	Maximal axial distance from LV midwall surface to origin	cm	Xm_LV
$x_{m,SEP}$	Maximal axial distance from SEP midwall surface to origin	cm	Xm_SEP
y_m	Radius of midwall junction circle	cm	ym

For given wall volumes and ventricular volumes, the geometry of the heart is solved such that equilibrium of radial and axial tensile forces is achieved at the junction margin (i.e., where the three wall segments meet forming ventricular cavities).

Tension in the midwall of each segment is calculated as a function of stress:

$$T_{m,\#} = \frac{V_{w,\#}\sigma_{SE,\#}}{2A_{m,\#}}\left(1 + \frac{z^2}{3} + \frac{z^4}{5}\right).$$

Axial and radial components of the tension are computed

$$T_{x,\#} = T_{m,\#}\frac{2x_{m,\#}y_m}{x_{m,\#}^2 + y_m^2}$$

$$T_{y,\#} = T_{m,\#}\frac{-x_{m,\#}^2 + y_m^2}{x_{m,\#}^2 + y_m^2}.$$

The four unknowns of the model—$x_{m,RV}$, $x_{m,LV}$, $x_{m,SEP}$, and y_m—are determined by satisfying the relations

$$V_{m,LV} = -V_{LV} - \frac{1}{2}V_{w,LV} - \frac{1}{2}V_{w,SEP} + V_{m,SEP}$$

$$V_{m,RV} = +V_{RV} - \frac{1}{2}V_{w,RV} - \frac{1}{2}V_{w,SEP} - V_{m,SEP}$$

$$T_{x,RV} + T_{x,LV} + T_{x,SEP} = 0$$

$$T_{y,RV} + T_{y,LV} + T_{y,SEP} = 0 \ .$$

Transmural pressures are computed

$$P_{trans,\#} = \frac{2T_{x,\#}}{y_m}$$

and the pressures in the cavities are computed

$$P_{LV} = -P_{trans,LV}$$

$$P_{RV} = +P_{trans,RV} \ .$$

Model Parameters:

Parameters defining the mass and geometry of the heart are identified from data on individual animals are defined in Table S3.2.

Table S3.2. Parameters in heart model.

Parameter	Definition	Value and units	Parameter name in code
$V_{w,LV}$	LV wall volume	Input (experimental data), mL	Vw_LV
$V_{w,SEP}$	Septal wall volume	(Input experimental data), mL	Vw_SEP
$V_{w,RV}$	RV wall volume	(Input experimental data), mL	Vw_RV
$A_{m,ref}^{LW}$	LV midwall reference surface area	adjustable, cm^2	Amref_LV
$A_{m,ref}^{SW}$	Septal midwall reference surface area	adjustable, cm^2	Amref_SEP
$A_{m,ref}^{RW}$	RV midwall reference surface area	adjustable, cm^2	Amref_RV
K_{SE}	Stiffness of series element	50000 mmHg/μm	Kse
η	Viscosity coefficient of myofibers	0.1 mmHg sec μm^{-1}	eta

4. Lumped-Parameter Cardiovascular Systems Model

Model Variables and Equations:

The lumped-parameter model illustrated in Fig. S3 is used to simulate pressures and flows in the systemic and pulmonary circuits. This simple lumped model invokes eight parameters representing: pulmonary resistance R_{pul}, pulmonary arterial and venous compliances C_{PA} and C_{PV}, systemic arterials resistances R_{Ao} and R_{sys}, systemic arterial compliance C_{SA}, and systemic venous compliance C_{SV}, systemic arterial resistance and aortic compliance C_{Ao}.
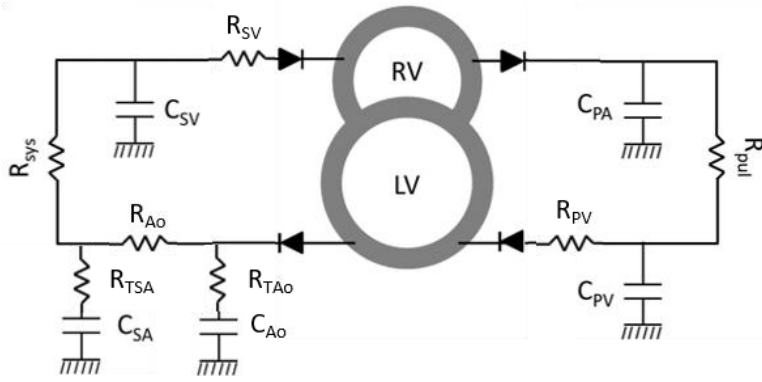
Fig. S3. Cardiovascular system (CVS) diagram. Adopted from Tewari et al. [3]. C_{PA}, C_{PV}, C_{SA}, C_{Ao}, and C_{SV} represent lumped compliances of pulmonary arteries, pulmonary veins, systemic arteries, aorta, and systemic veins. R_{pul}, R_{sys}, and R_{Ao} represent vascular resistances. The lumped-parameter representations of the systemic and pulmonary circuits are coupled to the TriSeg heart model [9], described below.

Flow through a resistive element is calculated

$$q = \frac{P_1 - P_2}{R}$$

where $P_1 - P_2$ is the pressure drop across the element, and R is the resistance. Pressure in a compliant/capacitive element is governed by

$$\frac{dP}{dt} = \frac{F_{in} - F_{out}}{C}$$

where $F_{in} - F_{out}$ is the rate of change of blood volume in the element.

Table S4.1 lists the variables of the cardiovascular systems model. These variables and Eqs. (4.1) and (4.2) are invoked in the MATLAB code Cardiovascularmechancis.m.

Table S4.1. Variables used in lumped-parameter cardiovascular model

Variable	Definition	Units used in code	Variable name in code
Cardiovascular system model state variables			
V_{LV}	Left ventricle volume	mL	V_LV
V_{RV}	Right ventricle volume	mL	V_RV
V_{SV}	Volume of systemic vein	mL	V_SV
V_{PV}	Volume of pulmonary vein	mL	V_PV
V_{SA}	Volume of systemic artery	mL	V_SA
V_{PA}	Volume of pulmonary artery	mL	V_PA
V_{Ao}	Volume of aorta	mL	V_Ao
Pressures computed from volume state variables			
P_{SV}	Systemic venous pressure	mmHg	P_SV
P_{PV}	Pulmonary venous pressure	mmHg	P_PV
P_{PA}	Pulmonary arterial pressure	mmHg	P_PA
P_{Ao}	Aortic pressure (proximal to TAC)	mmHg	P_Ao
P_{SA}	Systemic arterial pressure (distal to TAC)	mmHg	P_SA

Identification of Model Parameters:

Table S4.2 lists the parameters used in the lumped circulatory model.

14

Table S4.2. Parameter used in the CVS model

Parameter	Definition	Value and units used in code	Parameter name in code
C_{Ao}	Proximal aortic compliance	0.0022045 mL·mmHg^{-1}	C_Ao
C_{SA}	Systemic arterial compliance	0.0077157 mL·mmHg^{-1}	C_SA
C_{SV}	Systemic venous compliance	2.5 mL·mmHg^{-1}	C_SV
C_{PA}	Pulmonary arterial compliance	0.013778, mL·mmHg^{-1}	C_PA
C_{PV}	Pulmonary venous compliance	0.25 mL·mmHg^{-1}	C_PV
R_{Ao}	Proximal aortic resistance	2.5 mmHg·s·mL^{-1}	R_Ao
R_{sys}	Systemic vasculature resistance	adjustable, mmHg·s·mL^{-1}	R_SA
R_{SV}	Systemic veins resistance	0.25 mmHg·s·mL^{-1}	R_SV
R_{TAo}	Transmural aortic resistance	0.5 mmHg·s·mL^{-1}	R_tAo
R_{TSA}	Transmural systemic artery re-sistance	4 mmHg·s·mL^{-1}	R_tSA
R_{PA}	Pulmonary vasculature resistance	7.58 mmHg·s·mL^{-1}	R_PA
R_{PV}	Pulmonary veins resistance	0.25 mmHg·s·mL^{-1}	R_PV
R_{VLV}	Valve resistance	0.05 mmHg·s·mL^{-1}	R_VLV
R_{TAC}	Resistance of TAC	adjustable, mmHg·s·mL^{-1}	R_TAC

The systemic compliances (C_{SA}, C_{Ao}, C_{SV}) are fixed to produce a pulse pressure of roughly 33 mmHg for simulations of sham control rats. The pulmonary compliance (C_{PA}, C_{PV}) are fixed to roughly have the target value of 12 mmHg for the pulmonary pulse pressure. The resistance R_{Ao} is arbitrarily set to have a small pressure drop of 4 mmHg between the aorta and systemic arteries for cardiac output of the mean value of 95 mL per min. The systemic venous resistance R_{SV} is set so that the mean pressure in the systemic veins for sham control rats is 3 mmHg. The pulmonary resistances R_{PA} and R_{PV} are set to give a mean pulmonary arterial pressure of 21 mmHg and pulmonary venous pressure of 9 mmHg in the sham control rats.

The two parameters in the circulation model that are adjusted to match measured data on individual TAC and sham rats are R_{TAC} and R_{sys}. The resistance R_{TAC} represents the resistance across the transverse aortic constriction (TAC), and is set to zero in sham-operated rats. In TAC rats, the value of this resistance is obtained based on the pressure gradient across the TAC constriction estimated from ultrasound measurements of the velocity gradient. The pressure drop across the constriction is computed $\Delta P_{TAC} = \frac{1}{2}\rho(V_2{}^2 - V_1{}^2)$, where V_1 and V_2 are the velocities on either side of the TAC constriction. Given an estimated pressure drop the resistance is computed $R_{TAC} = \Delta P_{TAC}/CO$, where CO is the cardiac output. The systemic resistance R_{sys} is adjusted so that the mean arterial pressure (MAP) is maintained at 93.3 mmHg. (Model fitting procedures are detailed below in §5.)

5. Model fits and predictions associated with individual rats

Summary:

The cardiac energy metabolism and the whole-body cardiovascular mechanics model (which includes the heart model) are implemented as separate modules. These models are matched to data on an individual-animal basis. The cardiac energetics model takes as an input the myocardial ATP consumption rate, the measured metabolite pools levels, and the measured mitochondrial ATP synthesis capacity, and outputs the cytoplasm concentrations of phosphate metabolites. The cardiac mechanics code takes as an input the cytoplasmic concentrations of phosphate metabolites (namely, ATP, ADP, and Pi)

and computes as an output the ventricular end-systolic and end-diastolic volumes and arterial pressures to compare to measured data, and the myocardial ATP hydrolysis rate to use in the energetics module. The energetics and mechanics models are iteratively run until they simultaneously converge to a steady state at fit the target cardiovascular data.

Relationship between cross-bridge cycle and ATP hydrolysis rates:

The relationship between cross-bridge cycle rate and J_ATP, the rate myocardial oxygen consumption rate, is based on matching the myocardial oxygen consumption rate predicted by the model to that observed for the working rat heart. Duvelleroy et al. [10] report a mean oxygen consumption rate of approximately $MVO_2 = 0.313$ mL·(min·g)$^{-1}$ for work rates corresponding to resting state in blood perfused working hearts. Using a myocardial cell density (in terms of cardiomyocyte volume per unit mass of myocardium) of $\rho_{cell} = 0.694$ mL·g^{-1} and assuming a P/O$_2$ ratio (moles of ATP synthesized per mole of O$_2$ consumed) of 4.5 [11], we estimate a resting ATP hydrolysis rate of 1.33 mmol·(sec·L cell)$^{-1}$. (This value is approximately 2.5 times higher than the estimated resting ATP hydrolysis rate of to 0.547 mmol·(sec·L cell)$^{-1}$ for human myocardium [12].)

Simulations of the cardiovascular mechanics model predict an average cross-bridge cycling rate of 5.03 sec^{-1} for the mean sham-operated control rat. Assuming a fixed proportionality between cross-bridge cycling rate and myocardial ATP hydrolysis rate, yields a constant of proportionality of

ATP hydrolysis rate (mmol·(sec·L cell)$^{-1}$) = 0.264 (mmol·(L cell)$^{-1}$) × cross-bridge cycling rate (sec^{-1}).

If we assume that roughly 3/4 of the ATP consumed by the cardiomyocyte is consumed by the myosin ATPase, we estimate from this constant of proportionality the density of cross-bridge-forming units in a cardiomyocyte to be roughly 0.35 mmol per liter of cell. This density has been independently estimated to be 0.25 mmol per liter of cell for skeletal myocytes [13].

Fitting data on individual rats:

The full set of adjustable parameters invoked in the cardiovascular systems model is listed in Table S5.1. Certain adjustable parameters are set based on direct measurements and others are adjusted so that simulation outputs match measured data. Seven parameter values—$A_{m,ref}^{LW}$, $A_{m,ref}^{SEP}$, $A_{m,ref}^{RW}$, k_{force}, k_{SR}, R_{sys}, R_{TAC} are adjusted to fit model predictions to data from individual animals on end-systolic and end-diastolic volumes and estimated pressure drop across the aortic constriction in TAC animals, and to simultaneously maintain a fixed mean arterial pressure of 93.3 mmHg, to maintain end-diastolic sarcomere lengths in the LV, septum, and RV of 2.2 μm.

Ranges of estimated values of are listed in Table S5.1. Values of anatomical/geometric parameters representing heart masses and reference areas are higher in TAC rats than in sham control rats, reflecting hypertrophic remodeling.

The parameters k_{force} and k_{SR} govern the transition out of the inaccessible super-relaxed state in the calcium-activation model. Increased in the values of these parameters represent increased levels of phosphorylation of myosin binding protein C. Thus, the higher values of these parameters in TAC compared to sham animals represent a prediction that phosphorylation of this protein is increased in the TAC animals.

Simulations of TAC rats consistently show lower ATP, ADP, and CrP, reflecting reductions in the total adenine nucleotide and creatine pools. (See below.) Lower ADP levels require a compensatory increase in inorganic phosphate to maintain ATP synthesis.

The ranges of values of cross-bridge cycle rate, ATP hydrolysis rate, and end-systolic and end-diastolic volumes are listed in Table S5.2.

Table S5.1. Input arguments and adjustable parameters for cardiovascular mechanic model

Input variable	Variable name in code	Definition	Units used in code	Values
HR	HR	Heart rate	bpm	318.6-367 for sham 294-349 for TAC set to measured value
Vw,LV	Vw_LV	LV wall volume	mL	0.5642-0.8531 for sham 0.8628-1.2196 for TAC set as 2/3 of measured LV volume
Vw,SEP	Vw_SEP	Septal wall volume	mL	0.2821-0.4266 for sham 0.4314-0.6098 for TAC set as 1/3 of measured LV volume
Vw,RV	Vw_RV	RV wall volume	mL	0.282-0.3735 for sham 0.2495-0.6046 for TAC set as measured RV free wall volume
$A_{m,ref}^{LW}$	Amref_LV	LV midwall reference surface area	cm^2	1.7817-2.5086 for SHAM 2.3033-2.9151 for TAC adjusted to fit data
$A_{m,ref}^{SW}$	Amref_SEP	Septal midwall reference surface area	cm^2	1.0545-1.5271 for sham 1.2889-1.6134 for TAC adjusted to fit data
$A_{m,ref}^{RW}$	Amref_RV	RV midwall reference surface area	cm^2	2.9251-3.5298 for sham 3.1673-5.5305 for TAC adjusted to fit data
k_{force}	k_force	Model parameter for force dependent super relax transition	$N^{-1}m^{-2}$	(0.9285-3.6368)×10^{-3} for sham (1.6314-3.4283)×10^{-3} for TAC adjusted to fit data
k_{SR}	k1_SR	On rate constant for super relax state	s^{-1}	9.2565-36.2547 for sham 16.2632-34.1764 for TAC adjusted to fit data
R_{sys}	R_SA	Systemic vasculature resistance	mmHg·s·mL^{-1}	45.896-72.6107 for sham 50.5259-121.1621 for TAC adjusted to fit data
R_{TAC}	R_TAC	Resistance of TAC	mmHg·s·mL^{-1}	0 for sham 7.2614-20.5062 for TAC adjusted to fit data
MgATP_cytoplasm	MgATP	cytosolic [MgATP]	mmole·(l cytosol water)$^{-1}$	7.2308-9.4533 for sham 4.9443-9.0718 for TAC predicted from energetics model
MgADP_cytoplasm	MgADP	cytosolic [MgADP]	mmole·(l cytosol water)$^{-1}$	0.0408-0.0525 for sham 0.0235-0.0485 for TAC predicted from energetics model

| Pi_cyto | Pi | cytosolic total [Pi] | mmole·(l cyto-sol water)$^{-1}$ | 0.6132-1.92 for sham
1.808-2.621 for TAC
predicted from energetics model |

Table S5.2. Output arguments for cardiovascular mechanic model

variable	Definition	Units used in code	Values
rate_of_XB_turn-over_ave	Cross bridge cycling rate	sec^{-1}	3.9205-5.7314 for sham 2.8349-5.8006 for TAC
x_ATPase	ATP hydrolysis rate	mmole·sec^{-1}·(L cell)$^{-1}$	1.0339 - 1.5137 for sham 0.7487 - 1.5305 for TAC
EDLV	End diastolic left ventricular volume	mL	0.303-0.547 for sham 0.407-0.653 for TAC
ESLV	End systolic left ventricular volume	mL	0.092 – 0.235 for sham 0.137 - 0.424 for TAC
MAP	Mean arterial pressure	mmHg	93.3 for both TAC and sham

The set of input parameters invoked in the cardiovascular systems model is listed in Table S1.3. The input parameters TAN, CRtot, and Ox_capacity are all measured for each individual rat. The ATP hydrolysis rate (x_ATPase) is predicted by the mechanics model (see above). The age dependent relationship from Gao et el. [12] is used to estimate the total exchangeable phosphate (TEP):

$$TEP = P_0 - p\left((A_0 - TAN)/a\right)$$

where, $P_0 = 35.446$ mmol·(L cell)$^{-1}$, $A_0 = 10.26$ mmol·(L cell)$^{-1}$, are reference TEP and TAN values, $p = 0.283$ mmol·(L cell . year)$^{-1}$ and $a = 0.082$ mmol·(L cell . year)$^{-1}$ are the slopes of the relationships between mean TEP and mean TAN and age, respectively.

Output arguments from the energetics model, including the metabolite levels used in the mechanics model, are listed in Table S1.4.

Predictions associated with changing metabolic/energetic parameterization:

The predictions illustrated in Fig. 7 of the paper are made by replacing the parameters representing the metabolic state of sham control rats with those representing TAC rats and by replacing the parameters representing the metabolic state of TAC rats with those representing sham control rats.

For predictions of how mechanical function in sham rats changes when the metabolic profile is replaced with that of the average TAC rat (Fig. 7A), the input metabolic parameters are set to:

TAN = 0.006976 M

CRtot = 0.02303 M

TEP = 0.02411 M

Ox_capacity = 0.7482 (unitless)

Note that the above average TAC rat metabolite profile are based on n = 10 TAC rats. (TAC #7 was excluded for reasons described in main text.)

Given these values specifying the metabolic model, the blood volume, k_{force}, and k_{SR} are adjusted so that the model-predicted mean arterial pressure was 93.3 mmHg. In other words, it is assumed that

baseline cardiac output and system pressure are maintained at the original physiological levels via compensatory increases in preload and myosin binding protein C phosphorylation.

For predictions of how mechanical function in TAC rats changes when the metabolic profile is replaced with that of the average sham rat (Fig. 7B), the input metabolic parameters were set to:

TAN = 0.007624 M

CRtot =0.03027 M

TEP = 0.02635 M

Ox_capacity = 1 (unitless)

Given these values specifying the metabolic model, the blood volume, k_{force}, k_{SR} , and R_{sys} are adjusted so that the model-predicted mean arterial pressure is 93.3 mmHg and the predicted end-diastolic volume with mean sham metabolic parameters is equal to that of the original TAC rat. In other words, it was assumed that baseline system pressure and diastolic filling level are maintained at the original physiological levels via compensatory reduction in preload, myosin binding protein C phosphorylation, and systemic resistance.

6. Running the model

The simulation package consists of 5 MATLAB files:

1. *CardiovascualarMechanics.m:*
2. *dXdT_CardiovascularMechanics.m*
3. *EenergeticsModelScript.m*
4. *dXdT_energetics.m*
5. *TrisegEquations.m*

Values of all adjustable parameters are stored in spreadsheet files *"Adjustable_paramaters_table_rest.xlsx"* for the baseline simulations and *"Adjustable_parameters_table_SWAP.xlsx"* for simulations with replaced metabolic parameters.

The *CardiovascularMechanics.m* function is the main driver to run the mechanics model for a given animal. For instance, assigning the variable *"rat_number"* to 1 will execute simulations for SHAM rat number 1. Executing the script will load the parameters associated with this animal, run the cardiovascular systems model for 120 heart beats to attain a periodic steady state, and then plot the predicted left ventricular pressure, aortic pressure, and arterial pressure along with the left-ventricular pressure volume loop for this individual animal. The target end-diastolic and end-systolic volumes and the pressure drop across the TAC will be indicated by dashed lines in the figures. The model will compute the predicted cross-bridge cycling rate in the LV free wall and the associated ATP hydrolysis rate.

The energetics model for a given animal is called within the cardiovascular model. Executing this script will read the metabolic/energetic parameters associated with this animal and run the model to calculate the cytosolic metabolite levels. Note the ATPase hydrolysis rate for steady state is pre-identified and is listed in column 9 of the input *adjustable_parameters_table_rest.xlsx.*

The numbering for rats in the input data1.xlsx file is as follows: the first 8 rats are SHAM rats and rat number 9 is the mean sham rat; rat number 10 to 19 are the TAC rats (TAC rat# 7 is excluded). Therefore the first TAC rat is rat number 10 in the simulations. For example, to simulation the model for TAC rat #1 we need assign number 10 to the variable *"rat_numbers = 10" in the "CardiovascularMehanics.m"* and run the code.

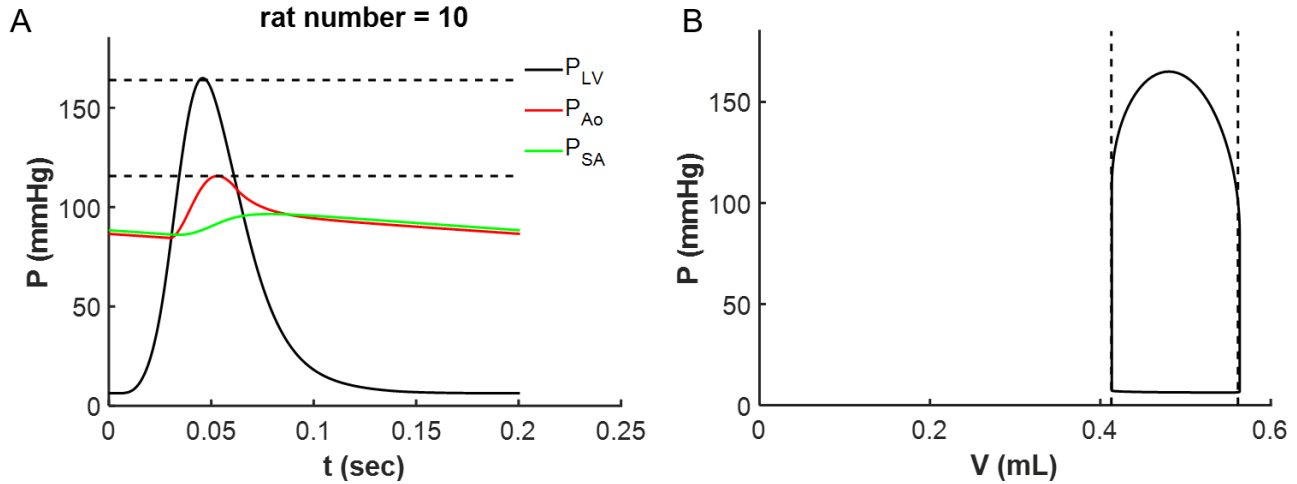The model will generate output shown below in Fig. S4.

Fig. S4. Model output for TAC rat #1.

In addition to the plots illustrated above, the running the model for this individual animal results in a predicted ATP hydrolysis rate of 0.748 mmole·sec^{-1}·(L cell)$^{-1}$. Note that the input ATP hydrolysis rate is the input parameters for the energetic model for this animal (column 9, rat number 10) of the adjustable variables in the input file "*adjustable_parameters_table_rest.xlsx*") is equal to this value. Also note that the predicted values for MgATP_cytoplasm, MgADP_cytoplasm, and Pi_cyto from the energetics model are equal to the associated input parameters for the mechanics model for this animal.

7. Glossary of model codes

EnergeticsModelScript.m: This function is used to compute the cellular energetics concentration variables for the myocardium, given input values of mitochondrial oxidative capacity, TAN, TEP, and CRtot metabolite pool values, and the rate of cellular ATP hydrolysis. The function computes the steady state of the cellular energetics model by simulating the model governed by the differential equations in *dXdT_energetics.m*.

dXdT_energetics.m: This function is an implementation of the Bazil et al. 2016 model of rat myocardial mitochondrial oxidative phosphorylation. The model has 29 state variables, listed in Table 1.1.

Cardiovascularmechanics.m: This function simulates the pressure and flows in the whole-body cardiovascular systems model of Fig. 1.1, governed by the five-compartment lumped-parameter cardiovascular systems model coupled to the Lumens et al. TriSeg heart model. The inputs to the model include the cytosolic metabolite concentrations predicted by *EnergeticsModelScript.m*. The outputs of the model are the myocardial ATP hydrolysis rate (used as an input for the energetics model) and the cardiovascular variables, EDLV, ESLV, MAP, rate of ATP cellular hydrolysis, to be compared to measurements for individual rats.

dXdT_cardiovascular_mechanics.m: This function is an implantation of the whole organ cardiovasucalar mechanics model. The model has 47 state variables listed in Tables S2.1, S3.1, and S4.1.

TriSeg.m: This function runs the TriSeg model equations to obtain estimates for initial value for ode solver and the associated algebraic equations.

References

1. Bazil, J.N., D.A. Beard, and K.C. Vinnakota, *Catalytic Coupling of Oxidative Phosphorylation, ATP Demand, and Reactive Oxygen Species Generation.* Biophys J, 2016. **110**(4): p. 962-71.

2. Vinnakota, K.C., et al., *Multiple ion binding equilibria, reaction kinetics, and thermodynamics in dynamic models of biochemical pathways.* Methods Enzymol, 2009. **454**: p. 29-68.

3. Tewari, S.G., et al., *Influence of metabolic dysfunction on cardiac mechanics in decompensated hypertrophy and heart failure.* J Mol Cell Cardiol, 2016. **94**: p. 162-175.

4. Tewari, S.G., et al., *Dynamics of cross-bridge cycling, ATP hydrolysis, force generation, and deformation in cardiac muscle.* J Mol Cell Cardiol, 2016. **96**: p. 11-25.

5. Campbell, K.S., P.M.L. Janssen, and S.G. Campbell, *Force-Dependent Recruitment from the Myosin Off State Contributes to Length-Dependent Activation.* Biophys J, 2018. **115**(3): p. 543-553.

6. Campbell, K.S., P.M.L. Janssen, and S.G. Campbell, *Force-Dependent Recruitment from the Myosin Off State Contributes to Length-Dependent Activation.* Biophysical Journal, 2018. **115**(3): p. 543-553.

7. Rice, J.J., et al., *Approximate model of cooperative activation and crossbridge cycling in cardiac muscle using ordinary differential equations.* Biophys J, 2008. **95**(5): p. 2368-90.

8. Janssen, P.M., L.B. Stull, and E. Marbán, *Myofilament properties comprise the rate-limiting step for cardiac relaxation at body temperature in the rat.* Am J Physiol Heart Circ Physiol, 2002. **282**(2): p. H499-507.

9. Lumens, J., et al., *Three-wall segment (TriSeg) model describing mechanics and hemodynamics of ventricular interaction.* Ann Biomed Eng, 2009. **37**(11): p. 2234-55.

10. Duvelleroy, M.A., et al., *Blood-perfused working isolated rat heart.* Journal of Applied Physiology, 1976. **41**(4): p. 603-607.

11. Wu, F., et al., *Phosphate metabolite concentrations and ATP hydrolysis potential in normal and ischaemic hearts.* The Journal of Physiology, 2008. **586**(17): p. 4193-4208.

12. Gao, X., D.G. Jakovljevic, and D.A. Beard, *Cardiac Metabolic Limitations Contribute to Diminished Performance of the Heart in Aging.* Biophys J, 2019. **117**(12): p. 2295-2302.

13. Barclay, C.J., R.C. Woledge, and N.A. Curtin, *Inferring crossbridge properties from skeletal muscle energetics.* Prog Biophys Mol Biol, 2010. **102**(1): p. 53-71.